

SPATIAL VARIABILITY OF THE FRONTAL ZONES AND ITS EDDIES
GENERATED IN THE NORWEGIAN SEAVladimir. S. Travkin^{*,1,2}  and Avelina F. Akhtyamova¹ ¹ Saint Petersburg State University, Saint Petersburg, Russia² N. N. Zubov's State Oceanographic Institute, Roshydromet, Moscow, Russia* **Correspondence to:** Vladimir S. Travkin, vtravkin99@gmail.com

Abstract: The Norwegian Sea is the meeting place of warm and salty Atlantic waters with cold and fresh Arctic waters. The thermal and haline frontal zones (FZs) formed as a result of this interaction are areas of increased horizontal gradients of physical, chemical, and biological parameters, and have a significant impact on regional circulation. Many mesoscale eddies are generated in the FZs which are actively involved in the eddy dynamics of the Norwegian Sea. The aim of this work is to analyze the spatio-temporal variability of the vertical structure of FZs in the Norwegian Sea, as well as the eddies that form within their boundaries. The work uses data from the oceanic reanalysis GLORYS12V1, as well as the Atlas of Mesoscale Eddies “Mesoscale Eddy Trajectory Atlas product META 3.2 DT” for the period 1993–2021. We analyze the average depth and thickness of FZs, the vertical distribution of their thermohaline gradients and areas. The work examines the seasonal and interannual variability of the volumes of thermal and haline FZs, the seasonal and interannual variability of mesoscale eddies, their spatial distribution, trajectories, and main parameters. In some areas, deepening of FZs has been established, and their thickness can reach 900 m. The presence of significant haline gradients in the layer of 250–750 m has been found, while thermal FZs can be traced vertically up to 1000 m compared with haline FZs. In some FZs, the interannual variability may exceed the seasonal one. The greatest variability of haline FZs can be traced in the autumn period, and the smallest – in the winter–spring. It is noticeable in the summer period that thermal FZs weaken. Eddies can leave the boundaries of the FZs and move away from the place of origin for hundreds of kilometers. The number and lifetime of cyclones exceed similar estimates for anticyclones, while anticyclones travel long distances compared to cyclones.

Keywords: frontal zones, mesoscale eddies, Norwegian sea, GLORYS12V1, META**Citation:** Travkin, V. S., and A. F. Akhtyamova (2023), Spatial Variability of the Frontal Zones and its Eddies Generated in the Norwegian Sea, *Russ. J. Earth. Sci.*, 23, ES3004, <https://doi.org/10.2205/2023es000844>

RESEARCH ARTICLE

Received: 22 November 2022

Accepted: 3 April 2023

Published: XX July 2023



Copyright: © 2023. The Authors. This article is an open access article distributed under the terms and conditions of the Creative Commons Attribution (CC BY) license (<https://creativecommons.org/licenses/by/4.0/>).

Introduction

The variability of the Global Ocean exists on all spatial and temporal scales, and its circulation is a complex system of vertical and horizontal movements covering the entire thickness and connecting the water masses between polar and tropical latitudes [Alexeev *et al.*, 2016; Richards and Straneo, 2015; Wunsch, 1992]. Oceanic frontal zones (FZs) are among the most common structures in the Global Ocean and represent areas of increased horizontal gradients in physical, chemical, and biological characteristics [Belkin, 2002; Fedorov, 1983; Gruzinov, 1986]. FZs have a significant impact on climate and ocean bioproductivity, and are the most efficient mechanism for mixing and transporting heat and salt through a vertically stable pycnocline [Brandini *et al.*, 2018; Chapman, 2014; Fedorov, 1983; Kushnir *et al.*, 2011; Russell *et al.*, 1999]. Due to their own instability, FZs are able to actively generate vortex disturbances [Fedorov, 1983]. FZs form in dynamically active regions where water masses of different characteristics and origins interact, and the

presence of a horizontal or vertical deformation field is the main condition for oceanic frontogenesis [Fedorov, 1983]. Baroclinic and barotropic instability, wind action, heat exchange with the atmosphere, as well as the influence of currents and tides increase the variability of FZs [Malinin and Gordeeva, 2009].

Other common structures of the Global Ocean are mesoscale eddies. Eddies contribute significantly to the total ocean bioproductivity, heat, mass, and sea ice transport [Belonenko et al., 2020; Mikaelyan et al., 2020]. It was shown by [Bashmachnikov et al., 2017] that the effect of the mesoscale eddy signal can be traced at a depth of several kilometers or even to the sea bottom. The spatial size of mesoscale eddies varies from the baroclinic Rossby deformation radius to a few hundreds of km, and their lifetime can reach the end of several years [Belonenko et al., 2020; Raj et al., 2016]. The main factor in the formation of mesoscale eddies is the baroclinic and barotropic instability of currents, which develops due to their close connection with the areas of FZs [Zhmur, 2011].

The Norwegian Sea has an area of about 1480 thousand km², and plays an important climatic and transport role, being a region of intense heat exchange between the ocean and the atmosphere, as well as a place of interaction between warm and salty Atlantic waters with cold and fresh Arctic waters (Figure 1) [Zalogin and Kosarev, 1999]. Such a circulation leads to the formation of significant thermohaline gradients in the regions of interaction between Arctic and Atlantic waters, which contributes to the active development of frontogenesis in the study area (Figure 1). Topographically, it consists of two large basins in the southwestern and northeastern parts – Norwegian (NB) and Lofoten (LB), respectively. The LB is an abyssal plain with an area of about 98.6 thousand km² and bounded by an isobath of 3000 m. LB is characterized by increased eddy activity and a large amount of warm and saline water in the central part, which makes it the largest thermal reservoir in the North Atlantic [Novoselova and Belonenko, 2020]. The quasi-permanent Lofoten Vortex (LV) is an intrapycnocline anticyclonic lens located in the central part of the LB (69.7°N, 3°E). Intense convection in winter, as well as merging with other mesoscale eddies, contributes to the constant regeneration and renewal of the LV, while topography features do not allow it to leave the LB [Ivanov and Korablev, 1995].

The Norwegian Atlantic Current is a direct extension of the North Atlantic Current and is the northern part of the meridional thermohaline circulation, which reduces the contrast between the meridional characteristics of the Atlantic water masses [Blindheim and Rey, 2004]. It consists of two large branches: the Norwegian Atlantic Frontal Current (NwAFC) skirts the LB border from the western part, while the Norwegian Atlantic Slope Current (NwASC) rounds the LB on the right (Figure 1). Along the Norwegian continental slope, there is a cold and fresh Norwegian Coastal Current (NCC), the formation of which is significantly influenced by river runoff.

In the Norwegian Sea, there are 5 climatic FZs of the climatic North Polar FZ separating the Arctic and Atlantic waters – these are the Faroe-Iceland FZ, East Iceland Current FZ; Jan Mayen (Arctic) FZ; Norwegian Coastal Current FZ and West Svalbard FZ (Figure 1) [Kostianoy and Nihoul, 2009; Kostianoy et al., 2004]. The article [Akhtyamova and Travkin, 2023] demonstrates the existence of a link between large-scale atmospheric fluctuations and the variability of the Norwegian Sea FZs. The North Atlantic Oscillation index (NAO) most significantly influences these FZs. NAO has several definitions, which are always associated with a meridional-oriented dipole structure in the atmospheric pressure field [Ambaum et al., 2001; Nesterov, 2013]. It is known that the negative phase of NAO leads to a weakening of the Jan Mayen FZ [Raj et al., 2019].

The aim of this article is a detailed study of the vertical structure of the Norwegian Sea FZs, as well as the study of mesoscale eddies that form in the FZs. Much attention has been paid to the spatial, seasonal and interannual variability of these structures. The paper gives detailed characteristics of the detected anticyclonic (AC) and cyclonic (C) eddies that are generated in FZs.

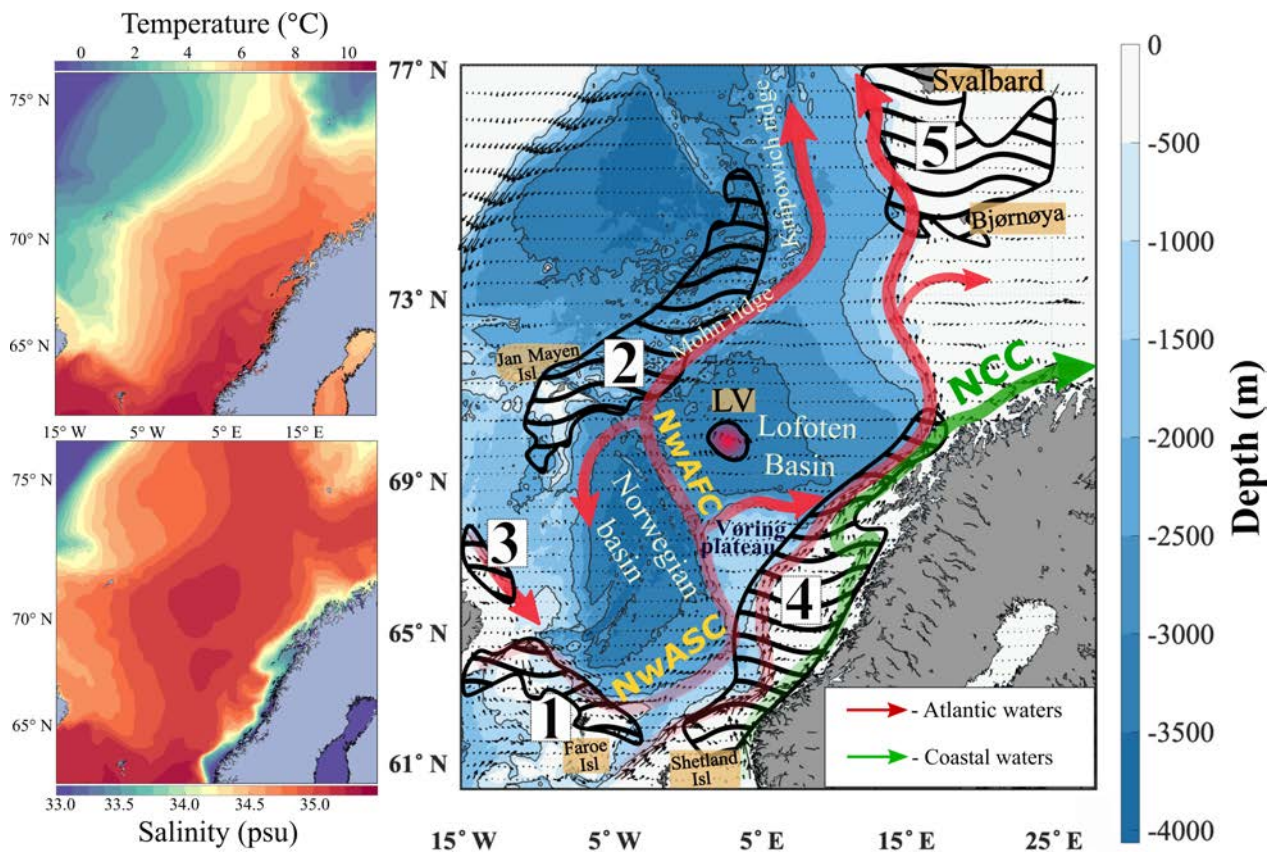


Figure 1. Averaged for 1993–2019 surface temperature and salinity fields (left) and a bathymetric map of the study area (right). Numerals show the Norwegian Sea FZs, hatching marks their boundaries: 1) Faroe-Iceland FZ; 2) Jan Mayen (Arctic) FZ; 3) FZ of the East Iceland Current; 4) FZ of the Norwegian Coastal Current; 5) FZ of Western Svalbard. Arrows show the main currents: NCC – the Norwegian Coastal Current, NwASC – the Norwegian Atlantic Slope Current, NwAFC – the Norwegian Atlantic Frontal Current. The location of the Lofoten Vortex is noted LV.

Data

GLORYS12V1

The work uses data on temperature, salinity, horizontal velocities, and sea surface height of the GLORYS12V1 global high-resolution ocean reanalysis (https://data.marine.copernicus.eu/product/GLOBAL_MULTIYEAR_PHY_001_030). The general ocean and sea ice circulation in the GLORYS12V1 is based on the NEMO platform, with conditions for the surface ocean model set using the ECMWF Era-Interim atmospheric reanalysis. The GLORYS12V1 uses satellite observations of sea surface anomalies, ocean surface temperatures, sea ice concentrations, and in situ vertical profiles of temperature and salinity. In addition to the Argo buoys, the reanalysis uses vertical temperature and salinity profiles obtained from observations of marine mammals. The results are assimilated using a reduced-order Kalman filter. The spatial resolution along the horizontal is $1/12^\circ$ (about 9.25 km at the equator and 4.5 km at subpolar latitudes), and the vertical resolution contains 50 levels with a step from 1 to 450 m, the time resolution is one day. The results of the works [Belonenko et al., 2021; Bosse and Fer, 2019; Romanov and Romanov, 2018] indicate a good agreement between the GLORYS12V1 and field measurements in the Norwegian Sea.

Mesoscale Eddy Trajectory Atlas DT (META 3.2 DT)

The work uses data from the Mesoscale Eddy Trajectory Atlas DT (META 3.2 DT) available on the AVISO+ portal (<https://www.aviso.altimetry.fr/en/data/products/value-added-products/global-mesoscale-eddy-trajectory-product/meta3-2-dt.html>) for the period 1993–2021.

The Atlas uses satellite data from all possible satellites in a certain period of time, which improves accuracy due to the difference in their periods and tracks. The principle of operation of the atlas algorithm is as follows. Initially, the absolute dynamic topography field is filtered, and large-scale variability is removed from it. Then, mesoscale eddies are detected in two steps. First, the closed contours of the absolute dynamic topography are scanned according to the specified criteria: if the contour corresponds to the criteria, then it is registered as a cyclone or anticyclone, otherwise, it is discarded [Pegliasco *et al.*, 2022]. In the next step, the center of the eddy, its boundaries, and the trajectory of motion are determined for each day. In addition, the Atlas contains daily information about the amplitude, area, radius, lifespan of the eddy, and other parameters. The eddies in the META 3.2 DT are divided into long-lived (lifespan ≥ 10 days) and short-lived (lifespan < 10 days). The period of 10 days is associated with the eddy detection method used in the algorithm, which is based on the imposition of effective contours [Pegliasco *et al.*, 2022].

Methods

To detect FZs in the Norwegian Sea, we use monthly temperature and salinity data for the time period 1993–2019. Seasonal averages were calculated according to the hydrological seasons: winter (January–March), spring (April–June), summer (July–September), and autumn (October–December). The algorithm for detecting the FZs is similar to the algorithm proposed by [Ozhigin *et al.*, 2016]. The module of the horizontal gradient was calculated by the formula:

$$|\text{grad } P| = \sqrt{\left(\frac{\partial P}{\partial x}\right)^2 + \left(\frac{\partial P}{\partial y}\right)^2},$$

where P is the value of the parameter (temperature, sea surface height or salinity), ∂x and ∂y are the step according to longitude and latitude. To identify the FZs, a selection condition was applied to the entire calculated data array: for temperature $|\text{grad } T| \geq 0.02$ °C/km, for salinity $|\text{grad } S| \geq 0.01$ psu/km, for sea surface height $|\text{grad } SSH| \geq 0.002$ psu/km. The selection criteria are based on the results of climatic averaging of hydrophysical fields and the choice of optimal values that also correspond to the studies of other authors. This method was successfully applied to determine the FZs of the Norwegian Sea in the work [Akhtyamova and Travkin, 2023].

To find the volume (V) of the FZs of the Norwegian Sea, we use the formula described in the work [Liu *et al.*, 2022]:

$$V = \sum_{k=1}^h \sum_{i=1}^n S_{i,k} \times h_k \times G_{\text{mask},k},$$

where h is the layer thickness (m), k is the layer number, $S_{i,k}$ is the cell area (m²), $G_{\text{mask},k}$ is a matrix in which FZs areas are equal to 1 and other zones are equal to 0. The cell area was calculated as the product of the distance between the closest points in latitude and longitude. Thus, if the horizontal gradient exceeded a threshold value in any layer, the volume of the FZ was calculated in that layer, considering the area and thickness of the layer.

Results

In most of the Norwegian Sea, the average for 1993–2019 the depths of thermal FZs do not exceed 100–300 m, while significant deepening is observed in the central and eastern parts of the LB (up to 600–700 m), as well as in the area of the Iceland-Faroe Ridge (up

to 1000 m) (Figure 2). In the Norwegian Sea, the average depth of the haline FZs does not exceed 100–200 m, increasing significantly only in small areas of the LB, NB, and Iceland-Faroe Ridge (up to 600–800 m). In the LB and near the Norwegian continental slope, thermal FZs can be traced up to 1000 m, and in the NB – up to 500–700 m. The largest thickness averaged for 1993–2019 period thermal FZs was found near the West Svalbard FZ (600–900 m) and the Jan Mayen FZ (about 500–800 m) (Figure 2). At the same time, haline FZs have a maximum thickness in the LB region, the Norwegian continental slope, and the Jan Mayen Ridge.

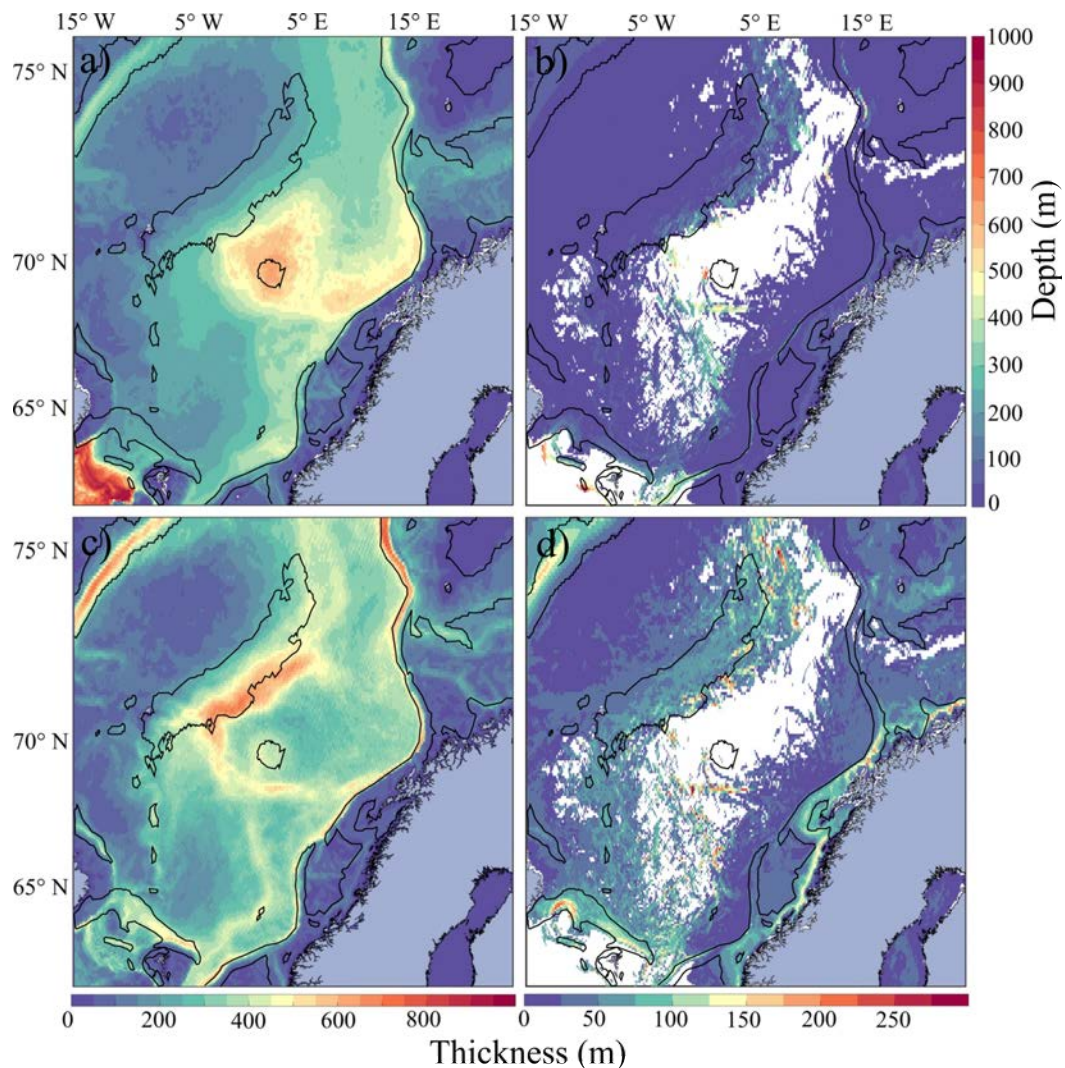


Figure 2. Averaged for the 1993–2019 period, the depth of thermal (a) and haline (b) gradients, as well as the thickness of thermal (c) and haline (d) gradients that exceed the corresponding threshold values. The contour indicates the boundaries of the FZs, defined as areas with a temporal frequency of the FZs $\geq 50\%$. Areas in which FZs were not found are marked in white.

It has been established that many FZs have strong gradients not only on the surface but also in the 250–750 m layer (Figure 3). It is noticeable that this intermediate maximum deepens to the north. The area of thermal FZs at first slightly increases with depth, and then gradually decreases, approaching zero at 1000 m. The exception here is the Norwegian Coastal Current FZ with a pronounced peak at 600 m, as well as the Faroe-Iceland FZ, extending to depths of more than 1000 m. In general, already at 500 m, most thermal FZs decrease in the area by 1.5–2 times relative to the maximum, while at 750 m, the area rarely exceeds 10–25% of the maximum. The area of haline FZs is significant for most FZs only on the surface, rapidly approaching zero with increasing depth (Figure 3).

The volume of thermal and haline FZs varies during a year, while the difference in values for adjacent months can reach tens of percent (Figure 4). In general, most FZs are characterized by one peak in the autumn–winter period, however, each FZ has its own seasonal fluctuations. Thus, the Faroe-Iceland thermal FZ is indicated by a maximum in September and a less pronounced peak in February. From February to March (from July to September), there is a significant decrease (increase) in the area of the FZ, while from March to July, the volume remains practically unchanged. The Jan Mayen thermal FZ is characterized by an increase in volume from March to September, while a strong reduction was observed from November to December and from February to March. The maximum (minimum) intensity is observed in September (March). The volume of thermal East Iceland Current FZ has a maximum in August and a minimum in April, with a significant magnification from May to August. The Norwegian Coastal Current FZ is characterized by the presence of two peaks close in intensity, in February and November. The maximum values of the volume of thermal West Svalbard FZ are observed in January, then there is an intense decrease from January to March, and the minimum was observed in August. It can be seen that the periods with above/below average values for thermal and haline FZs are quite similar, as, for example, in the case of the Jan Mayen FZ. Noticeably, the volume of

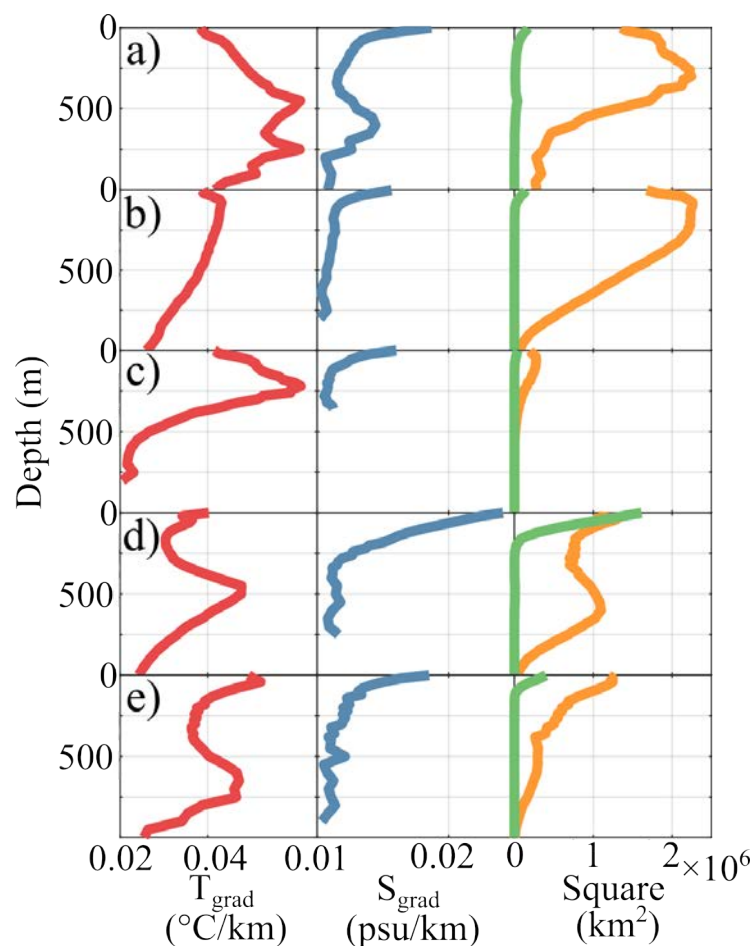


Figure 3. Vertical distribution of area-averaged FZs (see Figure 2) in the layer 0–1000 m temperature ($^{\circ}\text{C}/\text{km}$) (red) and salinity (psu/km) (blue) gradients for 1993–2019 period. Squares (km^2) of thermal (orange) and haline (green) FZs in the Norwegian Sea calculated within the boundaries of which are indicated in Figure 5. a) Faroe-Iceland FZ, b) East Iceland Current FZ; c) Jan Mayen (Arctic) FZ; d) Norwegian Coastal Current FZ; e) West Svalbard FZ.

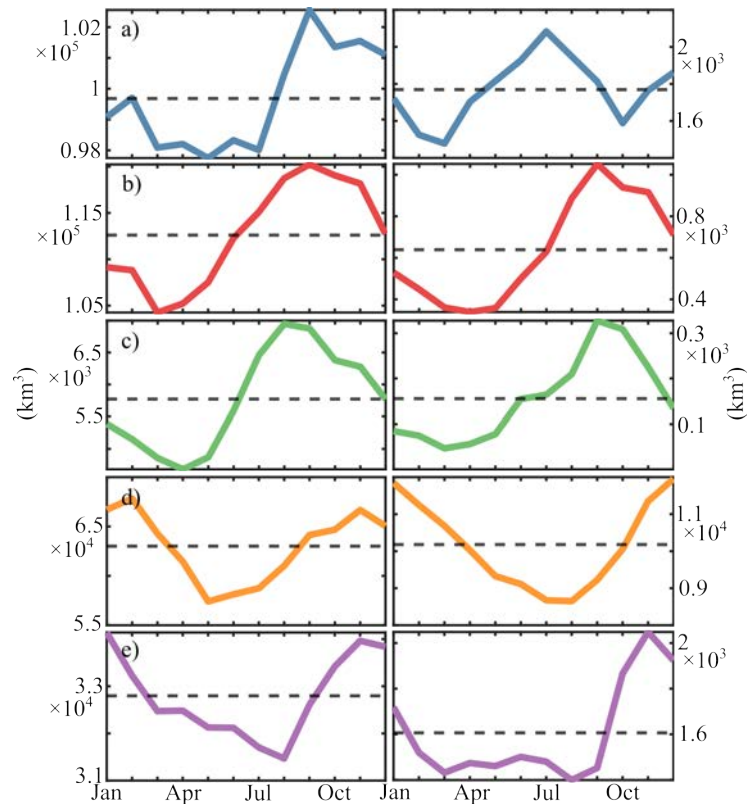


Figure 4. The volume of thermal (left) and haline (right) FZs by months, averaged over the 1993–2019 period, a) Faroe-Iceland FZ, b) East Iceland Current FZ; c) Jan Mayen (Arctic) FZ; d) Norwegian Coastal Current FZ; e) West Svalbard FZ. The dotted line shows the average values.

haline FZs is approximately 1–2 orders of magnitude smaller than the volume of similar thermal FZs, and the former are characterized by more pronounced variability.

Table 1 demonstrates that many thermal FZs have extremely weak seasonal fluctuations. Thus, fluctuations in the volume of the Faroe-Iceland FZ and the West Svalbard FZ are only 4–6% of the maximum values, while the greatest variability (26%) is observed in the East Iceland Current FZ. In summer, for most thermal FZs, a decrease in variability is noticeable. The range of seasonal variability of haline FZs varies in the range of 16–79% of the maximum values, while small fluctuations were recorded in the Faroe-Iceland FZ, Norwegian Coastal Current FZ, and West Svalbard FZ, and the largest in the East Iceland Current FZ. For haline FZs, the winter–spring period is characterized by the least variability, while in autumn the variability is usually mighty. Interannual fluctuations in the volume of thermal FZs are less pronounced than seasonal fluctuations. The least pronounced interannual variability of the thermal Jan Mayen FZ, as well as the West Svalbard FZ, while the variability is maximum in the Faroe-Iceland FZ and the East Iceland Current FZ. The haline FZs are characterized by pronounced interannual variability. It is maximum in the West Svalbard FZ and the Jan Mayen FZ, while the minimum values are recorded in the Norwegian Coastal Current FZ.

Many mesoscale cyclones and anticyclones are generated within the borders of FZs of the Norwegian Sea (Figure 5). Based on the data of the META 3.2 DT of mesoscale eddies, it can be seen that eddies of both types are able to move hundreds of kilometers from their place of birth, eventually dissipating into LB and NB. Moreover, the eddy motion trajectories are different for each FZ. It is noticeable that the East Iceland Current FZ is the least active in terms of eddy dynamics. Only in its northern part, the presence of separate eddies of both types can be traced, some of which move towards the NB. Numerous eddies are registered in the Faroe-Iceland FZ. Most of the eddies move eastward and southwestward, eventually dissipating near the southern border of NB, and in the Faroe-

Table 1. Mean values and root-mean-square of the volume of the thermal and haline FZs by season and year, normalized to 10^3 km^3

	Faroe-Iceland FZ	Jan Mayen (Arctic) FZ	East Iceland Current FZ	Norwegian Coastal Current FZ	West Svalbard FZ
Volume of thermal FZs					
Winter	99.96 ± 4.60	110.23 ± 10.17	5.44 ± 0.68	66.53 ± 4.50	33.73 ± 3.26
Spring	98.01 ± 4.47	105.66 ± 10.23	4.80 ± 0.84	61.05 ± 6.72	32.36 ± 3.34
Summer	98.93 ± 4.17	115.37 ± 9.27	6.33 ± 1.13	59.30 ± 5.60	31.76 ± 2.36
Autumn	101.82 ± 4.51	119.15 ± 10.01	6.51 ± 0.75	65.17 ± 6.20	33.33 ± 2.53
Year	99.68 ± 2.85	112.60 ± 7.74	5.77 ± 0.51	63.01 ± 3.52	32.80 ± 1.87
Volume of haline FZs					
Winter	1.70 ± 0.69	0.56 ± 0.52	0.10 ± 0.10	11.68 ± 1.28	1.72 ± 0.78
Spring	1.67 ± 0.82	0.35 ± 0.35	0.06 ± 0.07	10.01 ± 1.54	1.46 ± 0.57
Summer	1.99 ± 0.85	0.67 ± 0.54	0.18 ± 0.13	8.81 ± 1.47	1.46 ± 0.71
Autumn	1.72 ± 0.74	0.97 ± 0.59	0.29 ± 0.26	10.21 ± 1.48	1.79 ± 0.81
Year	1.77 ± 0.58	0.64 ± 0.39	0.16 ± 0.07	10.18 ± 0.99	1.61 ± 0.61

Shetland Channel. The Norwegian Coastal Current FZ is characterized by a pronounced movement of both types of eddies to the north and west. The long-lived AC eddies go around the Vøring Plateau from both sides, as a result of which some eddies become part of the NwAFC, while others become part of the NwASC. A rather significant part of eddies of both types moves into the eastern and northern parts of the LB. Near the Norwegian coast, a significant number of AC and, especially, C eddies move in south and east directions. For the western part of the West Svalbard FZ, the western direction of movement of eddies of both types is characteristic, with the northern direction of the middle currents. Quite many eddies move to the north, approaching close to Svalbard. With distance to the east, the trajectories of the motion of eddies change significantly. In that, the AC eddies change their direction to the opposite, to the east, while the cyclones begin to move to the southwest. The northern part of the Jan Mayen FZ is characterized by the movement of eddies in the northern and eastern directions. In the central and southern parts of the Jan Mayen FZ, most of the mesoscale eddies moving south and west, actively penetrating the western part of the LB and dissipating in the deepest part. Some long-lived cyclones reach the area where the LV is located. The direction of the trajectories of short-lived and long-lived eddies of the FZs generally coincides, although with slight differences.

It was found that the AC and C eddies have a significant difference in location (Figure 6). Thus, AC is characterized by being located in the western part of the West Svalbard FZ, in the eastern part of the Faroe-Iceland FZ, and in the western part of the Norwegian Coastal Current FZ. Whereas, the C eddies are located in the east of the West Svalbard FZ, in the southeast of the Norwegian Coastal Current FZ, and in the Faroe-Iceland FZ. The largest number of eddies of both types was observed in the Jan Mayen FZ and in the West Svalbard FZ. The number of C and AC eddies can reach 200 vortices per cell in them. It is noticeable that short-lived eddies leave the boundaries of the FZs much less frequently, moving mainly only within their boundaries.

Analysis of seasonal and interannual fluctuations in the number of eddies in the FZs for the presence of pronounced temporal variability (Figure 7). The average number of AC eddies per season can vary by 26% for long-lived eddies and by 24% for short-lived eddies. The winter–spring intensification of the FZs eddies is clearly visible. The interannual variability of the manifestation is about the presence of significant sensitive linear trends for eddies, and the number of AC eddies increases faster compared to C eddies. In general,

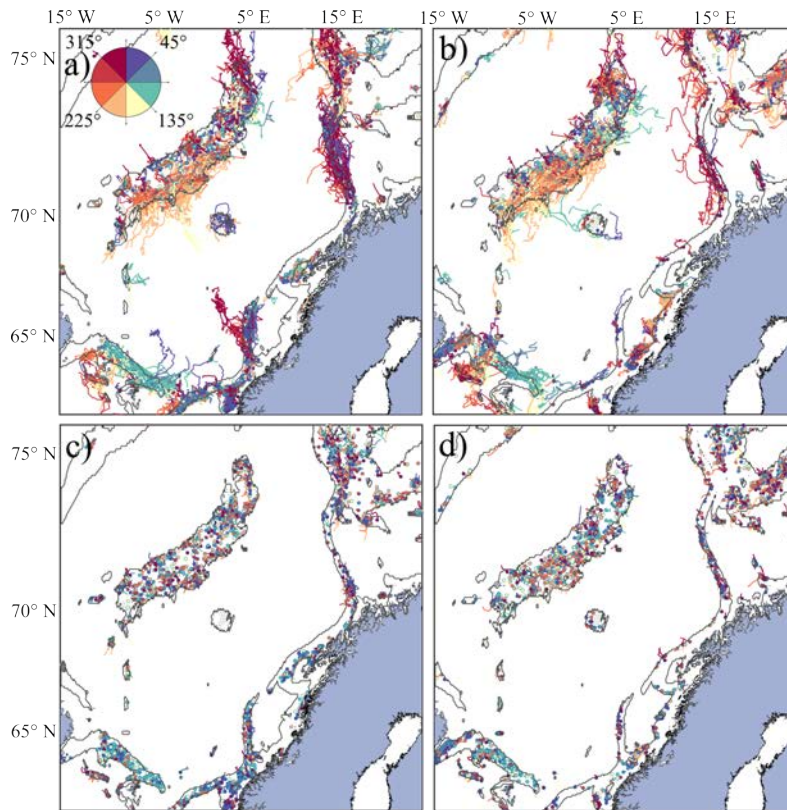


Figure 5. Trajectories of long-lived AC (a) and C (b), and short-lived AC (c) and C (d) eddies of the FZs for 1993–2021 period. The color shows the direction of the eddies, the dots indicate the places of their generation. Contours show the boundaries of the FZs.

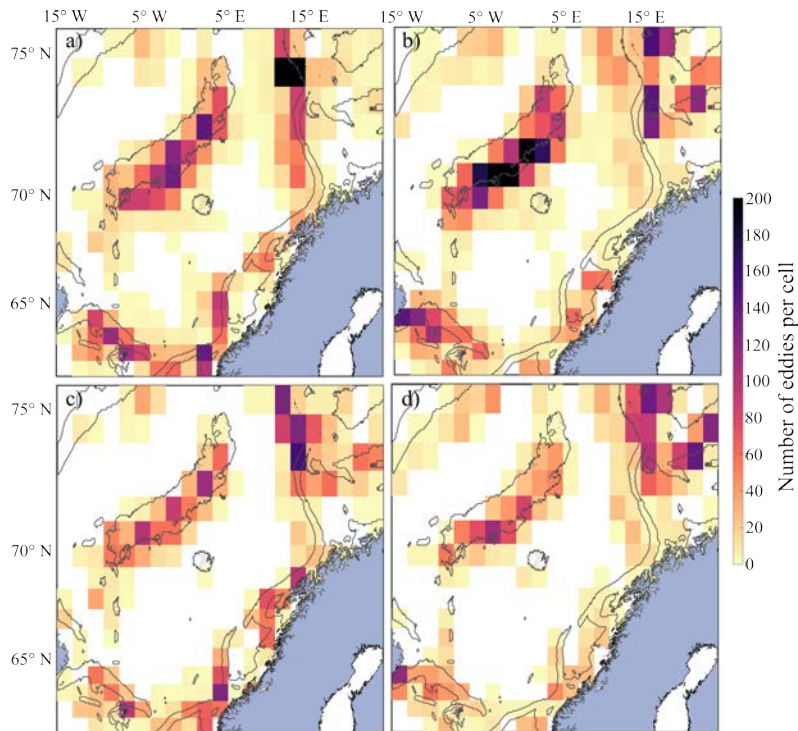


Figure 6. The number of long-lived anticyclones (a) and cyclones (b), short-lived anticyclones (c) and cyclones (d) per cell ($2^\circ \times 1^\circ$ in longitude and latitude). Contours show the boundaries of the FZs.

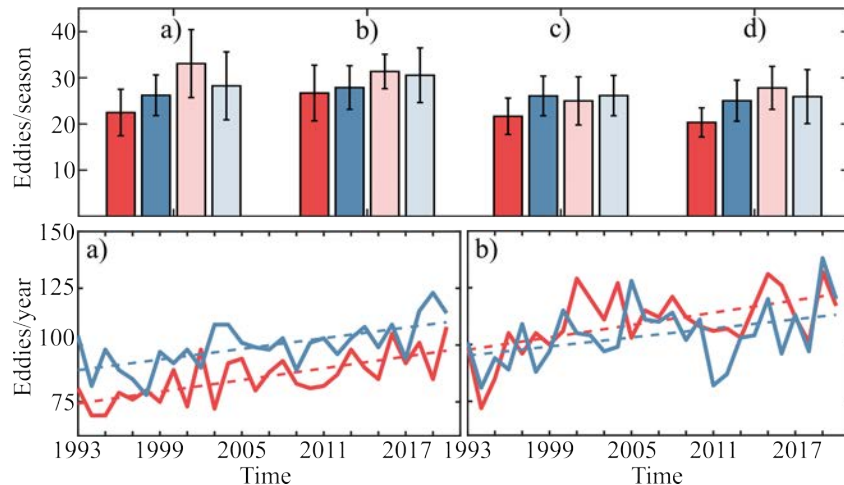


Figure 7. Top – the averaged number of long-lived AC (red), C (blue) and short-lived AC (light red) and C (light blue) FZs eddies by season: a) winter; b) spring; c) summer; d) autumn. Bottom – the number of FZs eddies per year for the 1993–2021 period: a) long-lived AC (red) and C (blue); b) short-lived AC (red) and C (blue).

the number of eddies varies significantly from year to year, reaching 25% between a couple of years and 75% between individual years.

Table 2 shows the parameters of the FZs eddies. Short-lived AC and C eddies significantly dominate in number, while C eddies are longer-lived. The cyclones are characterized by large spatial dimensions, while they vary in a wider range compared to the AC. On average, long-lived eddies have strong orbital speed, but weak movement per day, i.e. are more stationary. They have a longer life span, their average path length and displacement are ~ 7 and 3 times larger compared to similar values for short-lived eddies. In terms of the ratio of length to displacement, it is also noticeable that short-lived eddies have a more rectilinear trajectory.

Table 2. Mean and root-mean-square values of the main parameters of mesoscale eddies of FZs of the Norwegian Sea for 1993–2021 period

Parameter	AC		C	
	$t \geq 10$ days	$t < 10$ days	$t \geq 10$ days	$t < 10$ days
Amount	2462	3167	2841	2994
Lifetime period (days)	26.63	3.74	27.58	3.79
Area (km ²)	3083.7 ± 1470.6	1859.1 ± 552.6	3211.4 ± 1628.4	1987.6 ± 674.1
Amplitude (cm)	3.83 ± 0.99	3.96 ± 0.41	-2.33 ± 0.89	-1.88 ± 0.40
Radius (km)	33.89 ± 7.85	27.31 ± 3.78	34.00 ± 8.35	27.60 ± 4.29
Orbital speed (cm/s)	9.12 ± 1.56	7.28 ± 0.62	7.88 ± 1.47	6.26 ± 0.58
Movement per day (km/day)	5.34	5.78	5.40	5.90
Path (km)	138.52	20.56	148.12	21.41
Movement (km)	48.09	13.29	45.32	14.20

Summary

The average depth of FZs in the Norwegian Sea rarely exceeds 100–300 m, however, in the Faroe-Shetland Ridge and LB, it is significantly increased (Figure 2). This increase is associated with the isosteric deepening in the summer and autumn periods [Novoselova and Belonenko, 2020]. Eddy advection and bottom topography also play a significant role: with a strong slope of the relief, the angle of inclination of the isosteres increases,

which leads to an increase in thermohaline gradients. In addition to the eddy activity and bottom topography, the deep convection in the winter–spring period also contributes to the deepening of the depth of FZs [Fedorov *et al.*, 2021]. It has been established that in the central part of the LB in March, convection reaches its maximum, which leads to the subsidence of cold and fresh surface waters and an increase of mixed layer depth [Fedorov *et al.*, 2021; Travkin and Belonenko, 2020]. As a result, significant horizontal salinity gradients formed in the intermediate layer, and led to the creation of haline FZs.

The mean thickness of the thermal FZs is maximum in the West Svalbard FZ (600–900 m) and in the Jan Mayen FZ (about 500–800 m) (Figure 2). The thickness of haline FZs are maximal in the LB region, near the Norwegian continental slope, and the Jan Mayen Ridge. The main contribution to the formation of haline FZs in the continental slope is made by river runoff, whereas their formation is closely related to eddy activity in the LB and the Jan Mayen Ridge. It is known that in mesoscale eddies, vertical velocities can reach 0.8 m/day [Belonenko *et al.*, 2017; Koldunov and Belonenko, 2020]. The obtained high values of the thickness of FZs indicate an active circulation in the intermediate layer of the Norwegian Sea, which confirms to the existence of intense horizontal and vertical movements.

Significant temperature gradients in the FZs are traced not only on the surface, but also in the 250–750 m layer, and the intermediate maximum is observed to deepen when moving north (Figure 3). This distribution indicates intense subsidence of Atlantic waters to high depths and their major role in the frontogenesis of the Norwegian Sea. In general, with increasing depths, a significant decrease in the area of FZs occurs, while some thermal FZs can be traced down to 1000 m. The gradients and areas of haline FZs decrease noticeably faster compared to thermal FZs, for example, their area at a depth of 100–200 m is practically equal to zero.

The volume of FZs in the Norwegian Sea can vary both seasonally and yearly, also haline FZs are characterized by greater variability than thermal FZs (Figure 4). For most FZs, one peak is typical in the autumn–winter period, and the variability decreases in summer. The volume of haline FZs is 1–2 orders of magnitude smaller than the values of similar thermal FZs (Table 1).

Interannual and seasonal fluctuations of thermal FZs are maximum in the East Iceland Current FZ (18%) and minimal in the Faroe-Iceland FZ and West Svalbard FZ (4–6%) (Table 1). The seasonal variability of haline FZs is maximum in the East Iceland Current FZ (about 79%) and minimal in the Faroe-Iceland FZ, Norwegian Coastal Current FZ, and West Svalbard FZ (~16%). The interannual variability is pronounced in the haline FZs – it can exceed seasonal fluctuations in the West Svalbard FZ and the Jan Mayen FZ.

Each of the FZs has its own features of eddy propagation (Figure 5). Eddies of the FZs are capable of moving away from the place of generation for hundreds of kilometers and subsequently dissipating in the deep-water parts of the LB and NB. Anticyclones of the Faroe-Iceland FZ occur in NB at depths greater than 4000 m, while cyclones move along shallow depths (Figure 5). This feature is associated with the topographic effect described in [Carnevale *et al.*, 1991; Shchepetkin, 1995]. The eddy trajectories in different parts of the same FZ can vary significantly. For example, the eddies of the northern part of the Jan Mayen FZ propagate to the north and east, while in the central and southern parts, most of the generated eddies move to the south. Some of the long-lived cyclones of the Jan Mayen FZ dissipate in the region of the location of the LV, which highlights an important role of FZs in its regeneration (Figure 5). The number of eddies in the Jan Mayen FZ and West Svalbard FZ reaches 200 eddies per cell, that indicates a high intensity of eddy formation in these areas. The short-lived eddies leave the boundaries of the FZs much less frequently.

The eddies are characterized by strong seasonal and interannual variability, as well as winter–spring intensification (Figure 7). This intensification is associated with the baroclinic instability of the branches of the Norwegian Atlantic Current in winter, and with an increased rate of conversion of the average potential energy into available potential energy in the winter, which is a source for the formation of eddies [Raj *et al.*, 2016; Travkin

and Belonenko, 2019, 2021]. The interannual variability of the number of eddies has a significant positive linear trend, the strongest for anticyclones. A similar feature is also noted in [Travkin and Belonenko, 2021], where the presence of a positive significant linear trend in available potential energy associated with climate change in the North Atlantic is noted. There is also a similarity between the number of long-lived eddies in the FZs and the average annual AO and NAO indices from [Akhtyamova and Travkin, 2023]. The mechanism of this link is described by [Raj et al., 2019]. The number and lifetime of long-lived cyclones greatly exceed those for anticyclones, while long-lived anticyclones move to a larger distance, and make a significant contribution to the dynamics of the Norwegian Sea (Table 2). This fact is also noted in [Raj et al., 2016], where the high role of anticyclones in heat transfer is highlighted. It has been established that short-lived eddies move with a more rectilinear trajectory.

Acknowledgments. The authors acknowledge the support of Russian Science Foundation (RSF, project No. 22-27-00004).

References

- Akhtyamova, A. F., and V. S. Travkin (2023), Investigation of Frontal Zones in the Norwegian Sea, *Physical Oceanography*, 30(1), 62–77, <https://doi.org/10.29039/1573-160X-2023-1-62-77>.
- Alexeev, V. A., V. V. Ivanov, I. A. Repina, O. Y. Lavrova, and S. V. Stanichny (2016), Convective structures in the Lofoten Basin based on satellite and Argo data, *Izvestiya, Atmospheric and Oceanic Physics*, 52(9), 1064–1077, <https://doi.org/10.1134/s0001433816090036>.
- Ambaum, M. H. P., B. J. Hoskins, and D. B. Stephenson (2001), Arctic Oscillation or North Atlantic Oscillation?, *Journal of Climate*, 14(16), 3495–3507, [https://doi.org/10.1175/1520-0442\(2001\)014<3495:aoonao>2.0.co;2](https://doi.org/10.1175/1520-0442(2001)014<3495:aoonao>2.0.co;2).
- Bashmachnikov, I. L., M. A. Sokolovskiy, T. V. Belonenko, D. L. Volkov, P. E. Isachsen, and X. Carton (2017), On the vertical structure and stability of the Lofoten vortex in the Norwegian Sea, *Deep Sea Research Part I: Oceanographic Research Papers*, 128, 1–27, <https://doi.org/10.1016/j.dsr.2017.08.001>.
- Belkin, I. M. (2002), Front, in *Interdisciplinary Encyclopedia of Marine Sciences*, p. 433–436, Grolier Academic Reference.
- Belonenko, T., V. Zinchenko, S. Gordeeva, and R. P. Raj (2020), Evaluation of heat and salt transports by mesoscale eddies in the Lofoten Basin, *Russian Journal of Earth Sciences*, 20(6), 1–15, <https://doi.org/10.2205/2020es000720>.
- Belonenko, T. V., I. L. Bashmachnikov, A. V. Koldunov, and P. A. Kuibin (2017), On the vertical velocity component in the mesoscale Lofoten vortex of the Norwegian Sea, *Izvestiya, Atmospheric and Oceanic Physics*, 53(6), 641–649, <https://doi.org/10.1134/s0001433817060032>.
- Belonenko, T. V., V. A. Zinchenko, A. M. Fedorov, M. V. Budyansky, S. V. Prants, and M. Y. Uleysky (2021), Interaction of the Lofoten Vortex with a Satellite Cyclone, *Pure and Applied Geophysics*, 178(1), 287–300, <https://doi.org/10.1007/s00024-020-02647-1>.
- Blindheim, J., and F. Rey (2004), Water-mass formation and distribution in the Nordic Seas during the 1990s, *ICES Journal of Marine Science*, 61(5), 846–863, <https://doi.org/10.1016/j.icesjms.2004.05.003>.
- Bosse, A., and I. Fer (2019), Seaglider missions in the Norwegian Sea during the PROVULO project, <https://doi.org/10.21335/NMDC-980686647>.

- Brandini, F. P., P. M. Tura, and P. P. G. M. Santos (2018), Ecosystem responses to biogeochemical fronts in the South Brazil Bight, *Progress in Oceanography*, 164, 52–62, <https://doi.org/10.1016/j.pocean.2018.04.012>.
- Carnevale, G. F., R. C. Kloosterziel, and G. J. F. V. Heijst (1991), Propagation of barotropic vortices over topography in a rotating tank, *Journal of Fluid Mechanics*, 233, 119–139, <https://doi.org/10.1017/s0022112091000411>.
- Chapman, C. C. (2014), Southern Ocean jets and how to find them: Improving and comparing common jet detection methods, *Journal of Geophysical Research: Oceans*, 119(7), 4318–4339, <https://doi.org/10.1002/2014jc009810>.
- Fedorov, A. M., R. P. Raj, T. V. Belonenko, E. V. Novoselova, I. L. Bashmachnikov, J. A. Johannessen, and L. H. Pettersson (2021), Extreme Convective Events in the Lofoten Basin, *Pure and Applied Geophysics*, 178(6), 2379–2391, <https://doi.org/10.1007/s00024-021-02749-4>.
- Fedorov, K. N. (1983), *Physical nature and structure of oceanic fronts*, 296 pp., Hydrometeoizdat, Leningrad (in Russian).
- Gruzinov, V. M. (1986), *Hydrology of frontal zones of the World Ocean*, 272 pp., Hydrometeoizdat, Leningrad (in Russian).
- Ivanov, V. V., and A. A. Korablev (1995), Dynamics of an intrapycnocline lens in the Norwegian Sea, *Russian Meteorology and Hydrology*, 10, 32–37 (in Russian).
- Koldunov, A. V., and T. V. Belonenko (2020), Hydrodynamic Modeling of Vertical Velocities in the Lofoten Vortex, *Izvestiya, Atmospheric and Oceanic Physics*, 56(5), 502–511, <https://doi.org/10.1134/s0001433820040040>.
- Kostianoy, A. G., and J. C. J. Nihoul (2009), Frontal Zones in the Norwegian, Greenland, Barents and Bering Seas, in *Influence of Climate Change on the Changing Arctic and Sub-Arctic Conditions*, pp. 171–190, Springer Netherlands, https://doi.org/10.1007/978-1-4020-9460-6_13.
- Kostianoy, A. G., J. C. J. Nihoul, and V. B. Rodionov (2004), *Physical Oceanography of the Frontal Zones in Sub-Arctic Seas*, Elsevier Oceanography Series, 326 pp., Elsevier Science & Technology Books.
- Kushnir, V., V. Pavlov, A. Morozov, and O. Pavlova (2011), "Flashes" of chlorophyll-a concentration derived from in situ and remote sensing data at the Polar Front in the Barents Sea, *The Open Oceanography Journal*, 5(1), 14–21, <https://doi.org/10.2174/1874252101105010014>.
- Liu, Y., J. Wang, G. Han, X. Lin, G. Yang, and Q. Ji (2022), Spatio-temporal analysis of east greenland polar front, *Frontiers in Marine Science*, 9, 1–14, <https://doi.org/10.3389/fmars.2022.943457>.
- Malinin, V. N., and S. M. Gordeeva (2009), *Fishery oceanology of south-east Pacific*, vol. 1, 278 pp., RGGMU Publishing House (in Russian).
- Mikaelyan, A. S., A. G. Zatsepin, and A. A. Kubryakov (2020), Effect of Mesoscale Eddy Dynamics on Bioproductivity of the Marine Ecosystems, *Physical Oceanography*, 27(6), 590–618, <https://doi.org/10.22449/1573-160x-2020-6-590-618>.
- Nesterov, E. S. (2013), *North Atlantic Oscillation: Atmosphere and Ocean*, 144 pp., Triada, Moscow (in Russian).
- Novoselova, E. V., and T. V. Belonenko (2020), Isopycnal Advection in the Lofoten Basin of the Norwegian Sea, *Fundamental and Applied Hydrophysics*, 13(3), 56–67, <https://doi.org/10.7868/s2073667320030041> (in Russian).

- Ozhigin, V. K., V. A. Ivshin, A. G. Trofimov, A. L. Karsakov, and M. Y. Antsiferov (2016), *The Barents Sea water: structure, circulation, variability*, 260 pp., PINRO, Murmansk (in Russian).
- Pegliasco, C., A. Delepouille, E. Mason, R. Morrow, Y. Faugère, and G. Dibarboure (2022), META3.1exp: a new global mesoscale eddy trajectory atlas derived from altimetry, *Earth System Science Data*, 14(3), 1087–1107, <https://doi.org/10.5194/essd-14-1087-2022>.
- Raj, R. P., J. A. Johannessen, T. Eldevik, J. E. Ø. Nilsen, and I. Halo (2016), Quantifying mesoscale eddies in the Lofoten Basin, *Journal of Geophysical Research: Oceans*, 121(7), 4503–4521, <https://doi.org/10.1002/2016jc011637>.
- Raj, R. P., S. Chatterjee, L. Bertino, A. Turiel, and M. Portabella (2019), The Arctic Front and its variability in the Norwegian Sea, *Ocean Science*, 15(6), 1729–1744, <https://doi.org/10.5194/os-15-1729-2019>.
- Richards, C. G., and F. Straneo (2015), Observations of Water Mass Transformation and Eddies in the Lofoten Basin of the Nordic Seas, *Journal of Physical Oceanography*, 45(6), 1735–1756, <https://doi.org/10.1175/jpo-d-14-0238.1>.
- Romanov, A. A., and A. A. Romanov (2018), "Norwegian Sea – 97" *The major results of comprehensive experiment*, 311 pp., Space Research Institute of the Russian Academy of Sciences (IKI), Moscow (in Russian).
- Russell, R. W., N. M. Harrison, and G. L. Hunt (1999), Foraging at a front: hydrography, zooplankton, and avian planktivory in the northern Bering Sea, *Marine Ecology Progress Series*, 182, 77–93, <https://doi.org/10.3354/meps182077>.
- Shchepetkin, A. F. (1995), Interaction of turbulent barotropic shallow-water flow with topography, in *Proceedings of Hawaiian Winter Aha Huliko'a Workshop*, pp. 225–237, HI, Honolulu.
- Travkin, V. S., and T. V. Belonenko (2019), Seasonal variability of mesoscale eddies of the Lofoten Basin using satellite and model data, *Russian Journal of Earth Sciences*, 19(5), 1–10, <https://doi.org/10.2205/2019ES000676>.
- Travkin, V. S., and T. V. Belonenko (2020), Mixed layer depth in winter convection in the Lofoten Basin in the Norwegian Sea and assessment methods, *Hydrometeorology and Ecology, Proceedings of the Russian State Hydrometeorological University*, (59), 67–83, <https://doi.org/10.33933/2074-2762-2020-59-67-83> (in Russian).
- Travkin, V. S., and T. V. Belonenko (2021), Study of the Mechanisms of Vortex Variability in the Lofoten Basin Based on Energy Analysis, *Physical Oceanography*, 28(3), 294–308, <https://doi.org/10.22449/1573-160x-2021-3-294-308>.
- Wunsch, C. (1992), Decade-To-Century Changes In The Ocean Circulation, *Oceanography*, 5(2), 99–106.
- Zalagin, B. S., and A. N. Kosarev (1999), *Seas*, 400 pp., Mysl', Moscow (in Russian).
- Zhmur, V. V. (2011), *Mesoscale eddies of the Ocean*, 384 pp., GEOS, Moscow (in Russian).